Skin infection generates non-migratory memory CD8+ T$_{RM}$ cells providing global skin immunity

Xiaodong Jiang[1], **Rachael A. Clark**[1], **Luzheng Liu**[1], **Amy J. Wagers**[2], **Robert C. Fuhlbrigge**[1], and **Thomas S. Kupper**[1]

[1]Department of Dermatology and Harvard Skin Disease Research Center, Brigham and Women's Hospital, Harvard Medical School, Boston, MA 02115, USA

[2]Department of Stem Cell and Regenerative Biology, Harvard University, Howard Hughes Medical Institute, Harvard Stem Cell Institute, Joslin Diabetes Center, Boston, MA 02115, USA

Protective T cell memory has long been thought to reside in blood and lymph nodes, but very recently, the concept of immune memory in peripheral tissues mediated by resident memory T cells (T$_{RM}$) has been proposed [1–5]. Here we show that localized vaccinia virus (VACV) skin infection generates long-lived non-recirculating CD8$^+$ skin T$_{RM}$ that reside within the entire skin. These skin T$_{RM}$ are potent effector cells, and are superior to circulating central memory T cells (T$_{CM}$) at providing rapid long-term protection against cutaneous re-infection. We find that CD8$^+$ T cells are rapidly recruited to skin after acute VACV infection. CD8$^+$ T cell recruitment to skin is independent of CD4$^+$ T cells and IFN-γ, but requires the expression of E- and P-selectin ligands by CD8$^+$ T cells. Using parabiotic mice, we further show that circulating CD8$^+$ T$_{CM}$ and skin resident CD8$^+$ T$_{RM}$ are both generated after skin infection; however, CD8$^+$ T$_{CM}$ recirculate between blood and LN while T$_{RM}$ remain in skin. Cutaneous CD8$^+$ T$_{RM}$ produce effector cytokines and persist for at least 6 months after infection. Mice with CD8$^+$ skin T$_{RM}$ rapidly cleared a subsequent re-infection with VACV whereas mice with circulating T$_{CM}$ but no skin T$_{RM}$ showed greatly impaired viral clearance, indicating that T$_{RM}$ provide vastly superior protection. Finally, we show that T$_{RM}$ generated as a result of localized VACV skin infection reside not only in the site of infection, but also populate the entire skin surface and remain present for many months. Repeated re-infections lead to progressive accumulation of highly protective T$_{RM}$ in non-involved skin. These findings have important implications for our understanding of protective immune memory at epithelial interfaces with the environment, and suggest novel strategies for vaccines that protect against tissue tropic organisms.

CD8$^+$ T cells play a pivotal role in anti-viral immunity in target tissues[6–9]. We infected the skin of control, CD4$^{-/-}$, or CD4$^+$ T cell-depleted mice with VACV and assessed VACV-

specific pentamer^{+} CD8^{+} T cells[10]. Absence of CD4^{+} T cells did not impair either antigen-specific CD8^{+} T cell proliferation in dLN or subsequent accumulation in skin; in fact the latter was enhanced (Fig.1a, b). We then infected mice infused with OT-I (CD8^{+}) and OT-II (CD4^{+}) T cells with an ovalbumin-expressing VACV (VACV-Ova) [11]. After skin infection, both OT-I and OT-II cells proliferated similarly in dLN, and OT-I cells but not OT-II cells accumulated significantly in infected skin (though other CD4^{+} T cells showed some accumulation) (Supplementary Fig. 1 and Fig. 1c, d). Interestingly, OT-I cells accumulated in infected skin efficiently in the absence of either CD4^{+} T cells or IFN-γ (Fig. 1e, f), in contrast to a recently reported HSV vaginal infection model[12]. However, skin accumulation (but not LN proliferation) of OT-I cells from FucT IV/VII^{−/−} mice, which cannot make E- and P-selectin ligands, was significantly impaired (Fig. 1g, Supplementary Fig. 2a). Both E- and P-selectin were significantly upregulated in VACV infected skin (Supplementary Fig. 2b). Thus, CD8^{+} T cell accumulation in skin after VACV infection does not require CD4^{+} T cells or IFN-γ, but does require expression of E- and P-selectin ligands.

Murine models of viral infections of skin and other tissues have been useful in the study of T cell memory[13–16]. We explored the ability of CD8^{+} memory T cells generated by VACV infection to recirculate following resolution of the cutaneous infection. We infected with VACV the skin of mice infused with OT-I cells, and waited until complete resolution of the infection (30 days). At 30 days we could identify T_{CM} in LN and T_{EM} in skin (Supplementary Fig. 3a, b). We then surgically created parabiotic pairs between the infected mice and never-infected naïve mice that had not been given OT-I cells. Parabiotic pairs were maintained for 2, 4, 8, 12, and 24 weeks, at which point they were surgically separated for the analysis of VACV-specific OT-I T cells (Fig. 2a). Mice joined for 2 weeks had similar numbers of OT-I T_{CM} in the spleen and LN of both parabionts, indicating rapid recirculation and equilibration of T_{CM} (Fig. 2b, d). However, at 2, 4, or 8 weeks there were no OT-I T_{RM} in the skin of the unimmunized parabiont (Fig 2c, e). These early kinetics of T_{CM} recirculation and T_{RM} non-recirculation were confirmed by parabiotic mice that received no OT-I cells, using pentamer expression to identify VACV specific memory cells (Supplementary Fig. 4). OT-I T_{RM} were readily identified in the skin of previously infected parabionts and mice that had been infected in parallel but never joined. These OT-I T_{RM} represented a significant fraction of total skin cells (Fig. 2c), and persisted for long periods of time: 30% of skin CD8^{+} T cells at 12 weeks, and 15–20% of skin CD8^{+} T cells at 24 weeks. In contrast, naïve mice joined to previously infected mice had no OT-I T_{RM} in the skin, even after 24 weeks of parabiosis (Fig. 2c, e). Thus, skin T_{RM} persisted in skin for at least 6 months after infection and did not recirculate appreciably. T_{RM} and T_{CM} were further analyzed by FACS for expression of CD69, CD103, E- and P-selectin ligands, and production of IFN-γ and TNF-α upon activation. A subset of T_{RM} expressed Bcl-2, and T_{RM} lacked CD122 and CD127 (Supplementary Fig. 5). Immunofluorescence staining showed that many T_{RM} localize in epidermal and follicular epithelium, as reported in skin HSV infection[17], but also localize in the dermis (Fig. 2f).

To directly compare the ability of T_{CM} and T_{RM} to eliminate a subsequent VACV infectious challenge, we infused μMT mice with OT-I cells and infected them via skin with VACV-Ova. After 30 days, mice were joined parabiotically to naïve μMT mice for 8 weeks, and then surgically separated. The infected parabiont contained T_{CM} in both the spleen and LN

and T_{RM} within the skin, whereas the uninfected parabiont contained T_{CM} only in the spleen and LN (Fig. 2). At 2 weeks after separation, the skin of these mice was challenged with VACV-Ova, and assessed 6 days later for viral load (Fig. 3a). Despite the presence of abundant circulating OT-I T_{CM}, uninfected parabionts cleared virus only 30-fold more effectively than naïve mice (Fig. 3b). In contrast, the infected parabiont cleared the virus completely, 10^4-fold more effectively than the uninfected parabiont (Fig. 3b). Viral clearance was efficient even in mice treated with FTY720, a S1P inhibitor that blocks egress of T_{CM} from LN into blood[1] (Fig. 3b). To prove that this was not an artifact of OT-I cell transfer, we reproduced and extended the experiment in a parabiotic model not involving transfer of OT-I cells (Fig. 3c). Parabiotic pairs were separated at 4 weeks, challenged with VACV, and assessed for viral load at 6, 14, and 26 days after challenge. There were again striking differences in the ability of endogenous T_{RM} and T_{CM} to mediate viral clearance at days 6 (Fig. 3d) and 14 (Fig 3e), which began to normalize by day 26 (Fig. 3f). However, FTY720 treated T_{CM} mice are unable to clear virus even 26 days after infection, a time point by which naïve mice have cleared the skin infection (Fig. 3f), presumably by generating protective T_{RM}. Thus, while T_{CM} are superior to naïve T cells, they are inferior to T_{RM} at mediating rapid viral clearance from skin.

E- and P-selectin, CCL17, and ICAM-1 are expressed constitutively on the blood vessels of normal skin[18–20] and can support entry into uninflamed skin of T_{EM} generated by cutaneous VACV infection. To study this phenomenon, we infected the left ears of OT-I-loaded mice with VACV-Ova and then measured the accumulation of OT-I cells in both infected (left) and uninfected (right) ears. There was measurable accumulation of OT-I cells in both ears, with similar kinetics. The absolute number of OT-I cells was always higher in the infected ear, but even 30 days after infection, OT-I cells represented a measurable fraction of all cells present in the uninfected ear (Fig. 4a). Thus, VACV skin infection generates CD8+ T_{RM} that distribute to distant skin sites as well as the site of infection. The accumulation of OT-I T_{RM} in distant skin sites is increased further after multiple sequential infections to other sites of skin (Fig. 4b-d), suggesting that skin T_{RM} continue to accumulate throughout skin in response to repeated cutaneous infections at distant sites.

To determine if CD8+ T_{RM} in distant skin sites were protective as those at previously infected sites, we challenged μMT mice previously infected on one ear with a second VACV skin infection on both ears either 7 or 30 days after the initial infection. FYT720 was administered to limit the contribution of T_{CM} (Fig. 4e). Strikingly, at both day 7 and day 30, T_{RM} in distant skin sites dramatically reduced viral loads to levels comparable to those observed at the actual site of previous infection, indicating that these distant T_{RM} cells were highly effective at rapidly eliminating virus. In contrast, viral loads in the skin of i.p. immunized mice were between 10^3 and 10^4 higher at these time points (Fig. 4f, g). Thus, skin infection with VACV generates populations of T_{EM} that distribute to the entire skin surface, become T_{RM}, and mediate protection of the skin against re-infection with VACV in the absence of antibodies or T_{CM}.

T_{RM} have now been identified in the skin, gut, lung and brain in murine models[21–23] and human subjects in both health and in the setting of skin disease[4, 5, 24, 25]. We demonstrate that after VACV viral infection through skin, CD8+ T_{RM} are generated and distribute not

only to the site of infection but also throughout the entire skin surface. These $CD8^+$ T_{RM} produce effector cytokines, persist for many months, and are highly effective at rapidly controlling subsequent VACV skin infection. T_{RM} were orders of magnitude more effective than T_{CM} at controlling viral re-infection of the skin, at all time points examined in this study. The use of parabiotic mice allowed us to rigorously examine the tissue distribution and relative roles of T_{CM} and T_{RM} in VACV immune responses. The relatively minor role of $CD4^+$ T cells in VACV skin infection may reflect differences in immune responses to different viruses and/or infection of different tissues, as $CD4^+$ T cells are clearly more important in HSV infection [12, 26]. Moreover, $CD4^+$ T_{RM} cells predominate in human skin[24] and lung[25], and are enriched for memory cells specific for pathogens encountered through those tissues[27, 28].

Pathogens typically invade the host through epithelial interfaces with the environment. Our studies suggest that T_{EM} generated as a result of epithelial tissue infections accumulate as T_{RM} at both sites of infection as well as at distant sites within the same epithelial tissue, providing broad and long-lived protective T cell immunity against re-infection. A more complete understanding T_{RM} mediated immune memory should enhance our understanding of adaptive immunologic memory, influence rational vaccine design, and illuminate pathophysiology of human T cell mediated diseases.

METHODS

Mice

C57BL/6, $CD4^{-/-}$, IFN-$\gamma^{-/-}$ and μMT mice were purchased from The Jackson Laboratory. $Thy1.1^+$ $Rag^{-/-}$ OT-I, $CD45.1^+$ OT-II, FucT $IV/VII^{-/-}$ mice were housed at the animal facility of Harvard Institute of Medicine, Harvard Medical School. $Thy1.1^+$ $Rag^{-/-}$ OT-I mice were crossed with FucT $IV/VII^{-/-}$ mice to yield $Thy1.1^+$ FucT $IV/VII^{-/-}$ OT-I mice. OT-I and OT-II are T cell receptor-transgenic mice recognizing chicken ovalbumin residues 257–264 in the context of $H2K^b$ and 323–339 in the context of I-A^b, respectively. Animal experiments were performed in accordance with the guidelines set out by the Center for Animal Resources and Comparative Medicine at Harvard Medical School.

Viruses and Infections

Recombinant VACV (Western Reserve strain) and VACV-Ova were originally obtained from Dr. Bernard Moss (NIH, Bethesda, MD) and grown on Hela cells. Viral titres were determined using CV-1 cells and 2×10^6 PFU of VACV or VACV-Ova was used for epicutaneous infection by skin scarification (s.s.) or intraperitoneal (i.p.) injection, as described previously[29].

Parabiotic mice

Parabiosis surgery was performed as described elsewhere[30] with some modifications. Briefly, sex- and age-matched mouse partners were anesthetized to full muscle relaxation with ketamine and xylazine (10 μg/g) or with 2.5% avertin (15μl/g) by i.p. injection. The corresponding lateral aspects of mice were shaved and the excess hair was wiped off with alcohol prep pad. After skin disinfection by wiping with betadine solution and 70% ethanol

three times, two matching skin incisions were made from the olecranon to the knee joint of each mouse, and the subcutaneous fascia was bluntly dissected to create about 1/2 cm of free skin. The olecranon and knee joints were attached by a single 5-0 silk suture and tie, and the dorsal and ventral skins were approximated by staples or continuous suture. Betadine solution was used to cover the full length of the dorsal and ventral incision. The mice were then kept on heating pads and continuously monitored until recovery. 2.5 μg/g Flunixin was used for analgesic treatment by subcutaneous injection every 8–12 hours for 48 hours post operation. After an interval of the indicated weeks, parabiotic mice were surgically separated by a reversal of the above procedure for the next experiments.

Adoptive transfer and T cell depletion

Lymph nodes were collected from the naïve female Thy1.1$^+$ Rag$^{-/-}$ OT-I, CD45.1$^+$ OT-II, or Thy1.1$^+$ FucT IV/VII$^{-/-}$ OT-I mice at age of 6–8 weeks. OT-I or OT-II cells were purified by magnetic cell sorting using mouse CD8α$^+$ or CD4$^+$ T cell isolation kit (Miltenyi Biotec), respectively. 2×10^6 isolated OT-I and / or OT-II cells were then intravenously transferred to female recipient mice. In some experiments, OT-I and OT-II cells were labeled with carboxyfluorescein succinimidyl ester (CFSE) before co-transfer. To deplete CD4$^+$ T cells in vivo, the recipient mice were injected i.p. with 500 μg anti-CD4 (GK1.5) in 100 μl PBS 4 days and 1 day before and on day 2 and 5 post infection.

Preparation of cell suspensions

LN and spleen were harvested and mashed through a 70 μm nylon cell strainer to prepare cell suspensions. Red blood cells were lysed using lysing buffer. Skin tissue was removed after hair removal, chopped into small fragments and incubated in HBSS supplemented with 1 mg/ml collagenase A and 40 μg/ml DNase I at 37°C for 30 min. After filtrating through a 70 μm nylon cell strainer, cells were collected and washed thoroughly with cold PBS before staining.

Intracellular cytokine detection

The infected skin from memory OT-I-bearing mice was harvested at 35 days after infection, and single cell suspension was prepared as described above. In some cases, 2 months after s.s. with VACV-Ova, mice transferred with low (2×10^4) or high (2×10^6) number of OT-I cells were i.p. challenged with VACV-Ova. 5 days after challenge, splenocytes were prepared. Red blood cells were lysed using lysing buffer. Cells were then incubated with 2 μg/ml SINFEKL peptide of ovabulmin at the presence of Brefeldin A for 7 hours. Fc receptors were blocked with CD16/CD32 mAbs and intracellular IFN-γ, TNF-α and IL-2 staining was performed using Intracellular Cytokine Detection Kits (BD Bioscience) before flow cytometry.

Determination of viral load

Mice were challenged with 2×10^6 PFU VACV or VACV-Ova on the skin. In some cases, mice were simultaneously injected (i.p.) with 1 μg/g FTY720 each day. At indicated time points, viral load of skin was examined by quantitative real-time PCR, as described previously[29].

Isolation of mRNA and real-time PCR

Total RNA was extracted from homogenized skin tissue and cDNA was generated with iScript cDNA synthesis kit (Bio-Rad). Bio-Rad iCycler iQ Real-Time PCR Detection System (Bio-Rad) was used with the following settings: 45 cycles of 15 seconds of denaturation at 95°C, and 1 minute of primer annealing and elongation at 60°C. Real-time PCR was done with 1 µl cDNA plus 12.5 µl of 2× iQ™ SYBR Green Supermix (Bio-Rad) and 0.5 µl (10 µM) specific primers: mE-selectin 1 (5′-GGA CAC CAC AAA TCC CAG TCT G-3′) and mE-selectin 2 (5′- TCG CAG GAG AAC TCA CAA CTG G-3′); mP-selectin 1 (5′-AAG ATG CCT GGC TAC TGG ACA C-3′) and mP-selecin 2 (5′-CAA GAG GCT GAA CGC AGG TCA T-3′); mβ-actin 1 (5′-CAT TGC TGA CAG GAT GCA GAA GG-3′) and mβ-actin 2 (5′-TGC TGG AAG GTG GAC AGT GAG G-3′). All samples were run in duplicate and fold change of gene expression was calculated using the reference sample (naïve skin).

Antibodies and flow cytometry

The following anti-mouse antibodies were obtained from BD PharMingen: CD8a (53-6.7), Thy1.1 (OX-7), CD4 (L3T4), CD45.1 (A20), CD19 (1D3), CD16/CD32 (2.4G2), CD44 (IM7), CD62L (MEL-14), CD69 (H1.2F3), CD103 (M290), CD122 (TM-Beta 1), Bcl-2 (A19-3), $\alpha 4\beta 7$ (DATK32), IFN-γ (XMG1.2), TNF-α (MP6-XT22), IL-2 (JES6-5H4). Fluorescence-conjugated anti-mouse CD127 (A7R34) and PD-1 (RMP1-30) were purchased from eBioscience. PE-conjugated B8R$_{20-27}$/H-2K^b pentamers were obtained from ProImmune Ltd and pentamer$^+$ CD8$^+$ T cell staining was performed according to the protocol provided by company. E- or P-selectin ligand expression was examined by incubating cells with rmE-Selectin/Fc Chimera or rmP-Selectin/Fc Chimera (R&D System) in conjunction with APC-conjugated F(ab')$_2$ fragments of goat anti-human IgG F(c) antibody (Jackson Immunoresearch). Dead cells were excluded using 7-AAD staining. Data were analyzed on FACSCanto^{TM} Flow Cytometer using FACSDiva software.

Immunofluorescence Microscopy

1 cm tail containing the infected skin site from OT-I-bearing mice was harvested and deboned at 45 days after s.s. with VACV-Ova. The skin was collected and embedded in OCT (Tissue-Tek; Sakura) and frozen at −80°C. Skin sections were performed on a cryostat (Leica CM1850 UV) at 6-µm thickness and air-dried for 6–8 hours. Sections were then fixed in −20°C acetone for 5 min, rehydrated with PBS properly, and blocked with 2% FCS in PBS for 15 min at room temperature (RT, 20°C). After staining with Thy1.1-PE (1:200) in PBS for 1 hour at RT, sections were rinsed 3 times (5 min/time) with TBS-tween 20 by properly shaking and mounted with DAPI Fluoromount-G (Southern Biotech, Alabama, USA). Images were acquired with a Nikon Eclipse E600 microscope and processed using SPOTSOFTWARE (version 4.6, Diagnostic Instruments, Inc.).

Statistical analysis

Statistical significance in values between experimental groups was determined by one-way analysis of variance (ANOVA) followed by Tukey post-test. $P<0.05$ was considered statistically significant.

Supplementary Material

Refer to Web version on PubMed Central for supplementary material.

Acknowledgements

References

1. Liu L, et al. Epidermal injury and infection during poxvirus immunization is crucial for the generation of highly protective T cell-mediated immunity. Nat Med. 2010; 16:224–227. [PubMed: 20081864]

2. Bevan MJ. Memory T cells as an occupying force. Eur J Immunol. 2011; 41:1192–1195. [PubMed: 21469134]

3. Sheridan BS, Lefrançois L. Regional and mucosal memory T cells. Nat Immunol. 2011; 131:485–491. [PubMed: 21739671]

4. Boyman O, et al. Spontaneous development of psoriasis in a new animal model shows an essential role for resident T cells and tumor necrosis factor-α. J Exp Med. 2004; 199:731–736. [PubMed: 14981113]

5. Conrad C, et al. α1β1 integrin is crucial for accumulation of epidermal T cells and the development of psoriasis. Nat Med. 2007; 13:836–842. [PubMed: 17603494]

6. Bevan MJ. Helping the CD8(+) T-cell response. Nat Rev Immunol. 2004; 4:595–602. [PubMed: 15286726]

7. Antia R, Ganusov VV, Ahmed R. The role of models in understanding CD8+ T-cell memory. Nat Rev Immunol. 2005; 5:101–111. [PubMed: 15662368]

8. Kaech SM, Wherry EJ. Heterogeneity and cell-fate decisions in effector and memory CD8+ T cell differentiation during viral infection. Immunity. 2007; 27:393–405. [PubMed: 17892848]

9. Lefrançois L, Obar JJ. Once a killer, always a killer: from cytotoxic T cell to memory cell. Immunol Rev. 2010; 235:206–218. [PubMed: 20536565]

10. Freyschmidt EJ, et al. Skin inflammation arising from cutaneous regulatory T cell deficiency leads to impaired viral immune responses. J Immunol. 2010; 185:1295–1302. [PubMed: 20548030]

11. Sanz P, Moss B. Identification of a transcription factor, encoded by two vaccinia virus early genes, that regulates the intermediate stage of viral gene expression. Proc Natl Acad Sci U S A. 1999; 96:2692–2697. [PubMed: 10077573]

12. Nakanishi Y, Lu B, Gerard C, Iwasaki A. CD8(+) T lymphocyte mobilization to virus-infected tissue requires CD4(+) T-cell help. Nature. 2009; 462:510–513. [PubMed: 19898495]

13. Wakim LM, Waithman J, van Rooijen N, Heath WR, Carbone FR. Dendritic cell-induced memory T cell activation in nonlymphoid tissues. Science. 2008; 319:198–202. [PubMed: 18187654]

14. Masopust D, Vezys V, Marzo AL, Lefrançois L. Preferential localization of effector memory cells in nonlymphoid tissue. Science. 2001; 291:2413–2417. [PubMed: 11264538]

15. Lefrançois L. Development, trafficking, and function of memory T-cell subsets. Immunol Rev. 2006; 211:93–103. [PubMed: 16824120]

16. Klonowski KD, et al. Dynamics of blood-borne CD8 memory T cell migration in vivo. Immunity. 2004; 20:551–562. [PubMed: 15142524]

17. Gebhardt T, et al. Different patterns of peripheral migration by memory CD4+ and CD8+ T cells. Nature. 2011; 477:216–219. [PubMed: 21841802]

18. Chong BF, Murphy JE, Kupper TS, Fuhlbrigge RC. E-selectin, thymus- and activation-regulated chemokine/CCL17, and intercellular adhesion molecule-1 are constitutively coexpressed in dermal microvessels: a foundation for a cutaneous immunosurveillance system. J Immunol. 2004; 172:1575–1581. [PubMed: 14734737]

19. Weninger W, et al. Specialized contributions by alpha(1,3)-fucosyltransferase-IV and FucT-VII during leukocyte rolling in dermal microvessels. Immunity. 2000; 12:665–676. [PubMed: 10894166]

20. Jiang X, Campbell JJ, Kupper TS. Embryonic trafficking of γδ T cells to skin is dependent on E/P selectin ligands and CCR4. Proc Natl Acad Sci U S A. 2010; 107:7443–7448. [PubMed: 20368416]

21. Gebhardt T, et al. Memory T cells in nonlymphoid tissue that provide enhanced local immunity during infection with herpes simplex virus. Nat Immunol. 2009; 10:524–530. [PubMed: 19305395]

22. Masopust D, et al. Dynamic T cell migration program provides resident memory within intestinal epithelium. J Exp Med. 2010; 207:553–564. [PubMed: 20156972]

23. Wakim LM, Woodward-Davis A, Bevan MJ. Memory T cells persisting within the brain after local infection show functional adaptations to their tissue of residence. Proc Natl Acad Sci U S A. 2010; 107:17872–17879. [PubMed: 20923878]

24. Clark RA, et al. The vast majority of CLA+ T cells are resident in normal skin. J Immunol. 2006; 176:4431–4439. [PubMed: 16547281]

25. Purwar R, et al. Resident memory T cells (T(RM)) are abundant in human lung: diversity, function, and antigen specificity. PLoS One. 2011; 6:e16245. [PubMed: 21298112]

26. Lund JM, Hsing L, Pham TT, Rudensky AY. Coordination of early protective immunity to viral infection by regulatory T cells. Science. 2008; 320:1220–1224. [PubMed: 18436744]

27. Román E, et al. CD4 effector T cell subsets in the response to influenza: heterogeneity, migration, and function. J Exp Med. 2002; 196:957–956. [PubMed: 12370257]

28. Romani L. Immunity to fungal infections. Nat Rev Immunol. 2011; 11:275–288. [PubMed: 21394104]

29. Liu L, Fuhlbrigge RC, Karibian K, Tian T, Kupper TS. Dynamic programming of CD8+ T cell trafficking after live viral immunization. Immunity. 2006; 25:511–520. [PubMed: 16973385]

30. Wagers AJ, Sherwood RI, Christensen JL, Weissman IL. Little evidence for developmental plasticity of adult hematopoietic stem cells. Science. 2002; 297:2256–2259. [PubMed: 12215650]
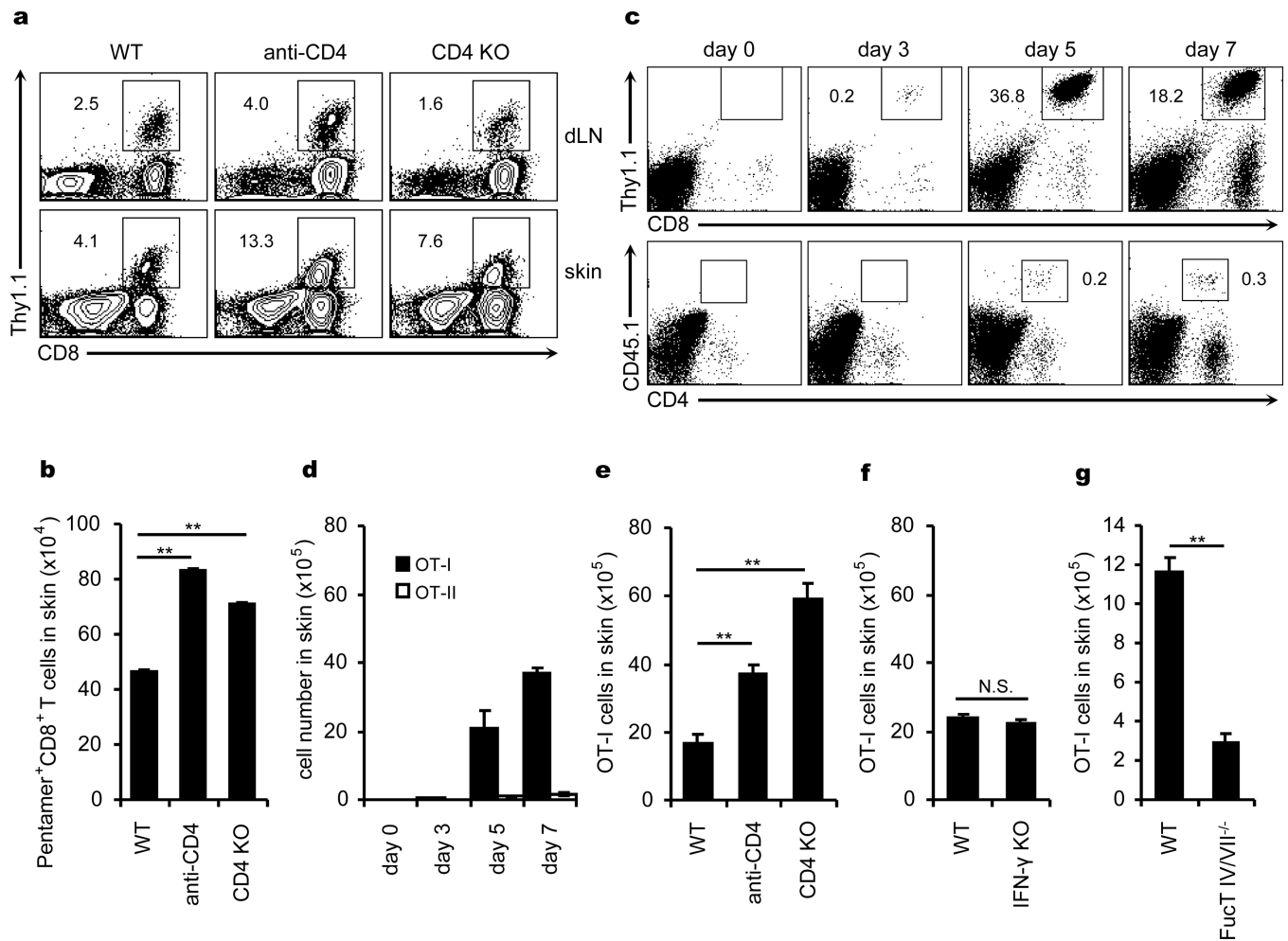
Figure 1. CD4+ T cells and IFN-γ are not required for acute recruitment of CD8+ T cells to VACV-infected skin

Pentamer+ CD8+ T cells in dLN and infected skin 7 days after VACV infection. **a**, The percentages of pentamer+ CD8+ T cells are shown (excluding CD19+ cells before flow cytometry analysis). **b**, The numbers of pentamer+ CD8+ T cells in infected skin. **c, d**, The kinetic infiltration of Thy1.1+ OT-I and CD45.1+ OT-II cells to infected skin after their co-transfer to naive mice. **e-g**, The numbers of OT-I cells in infected skin 7 days after infection in the absence of CD4, IFN-γ or FucT IV/VII, respectively. All data above are representative of at least three independent experiments (n = 5 mice/time point/group). **b**, **d-g**, Error bars, s.e.m.; **, P<0.01; N.S., not significant. WT, wild-type; KO, knockout; dLN, draining lymph node.
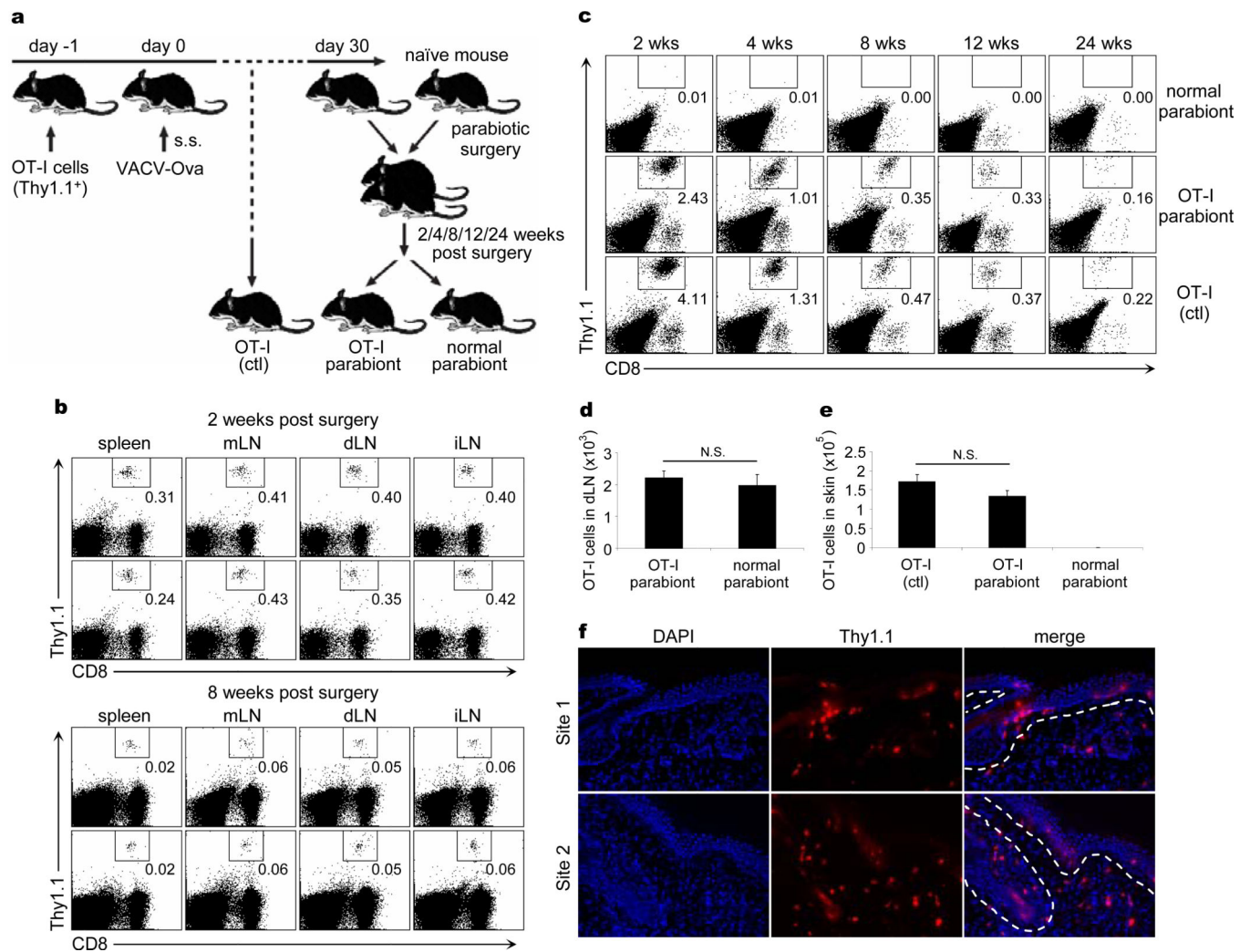
Figure 2. CD8$^+$ T$_{CM}$ re-circulate quickly between parabiotic mice, but skin CD8$^+$ T$_{RM}$ remain in place long term
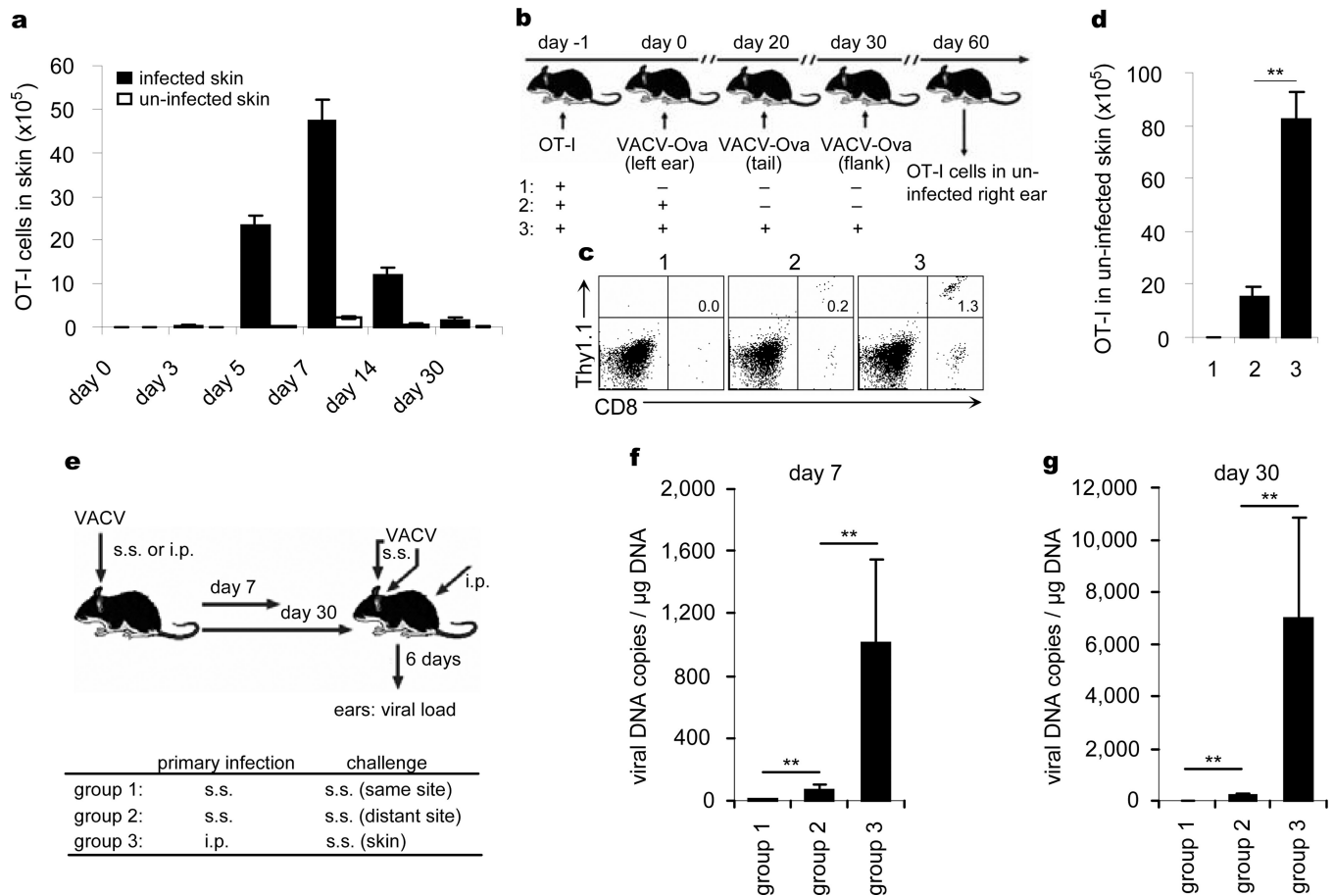
a, 2×10^6 Thy1.1$^+$ OT-I cells were intravenously transferred into Thy1.2$^+$ mice 1 day prior to 2×10^6 PFU VACV-Ova skin scarification. 30 days after infection, OT-I-bearing mice were joined surgically with naïve Thy1.2$^+$ mice to create parabiotic mice. At indicated time points after surgery, parabiotic mice were separated and lymphoid tissues and skin were harvested to examine OT-I cells. **b**, The percentages of memory OT-I cells in the indicated lymphoid tissues between parabiotic mice 2 and 8 weeks after surgery were examined. **c**, The percentages of OT-I T$_{RM}$ in the skin of parabiotic and control mice over time were also examined. **d**, The numbers of OT-I T$_{CM}$ in dLN of parabiotic mice 8 weeks after surgery. **e**, The numbers of OT-I T$_{RM}$ in the skin of parabiotic and control mice 8 weeks after surgery. **b-e**, Data are representative of three independent experiments (n = 5 mice/time point/group). **d,e**, Error bars, s.e.m.; N.S., not significant. **f**, Immunofluorescence of OT-I cells in infected skin sites 45 days after infection. Sections were stained for nuclei (DAPI, blue) and Thy1.1 (red). n = 15 sections from 5 mice. Two representative sites are shown. mLN, mesenteric lymph node; dLN, draining lymph node; iLN, inguinal lymph node; DAPI, 4′,6-diamidino-2-phenylindole.
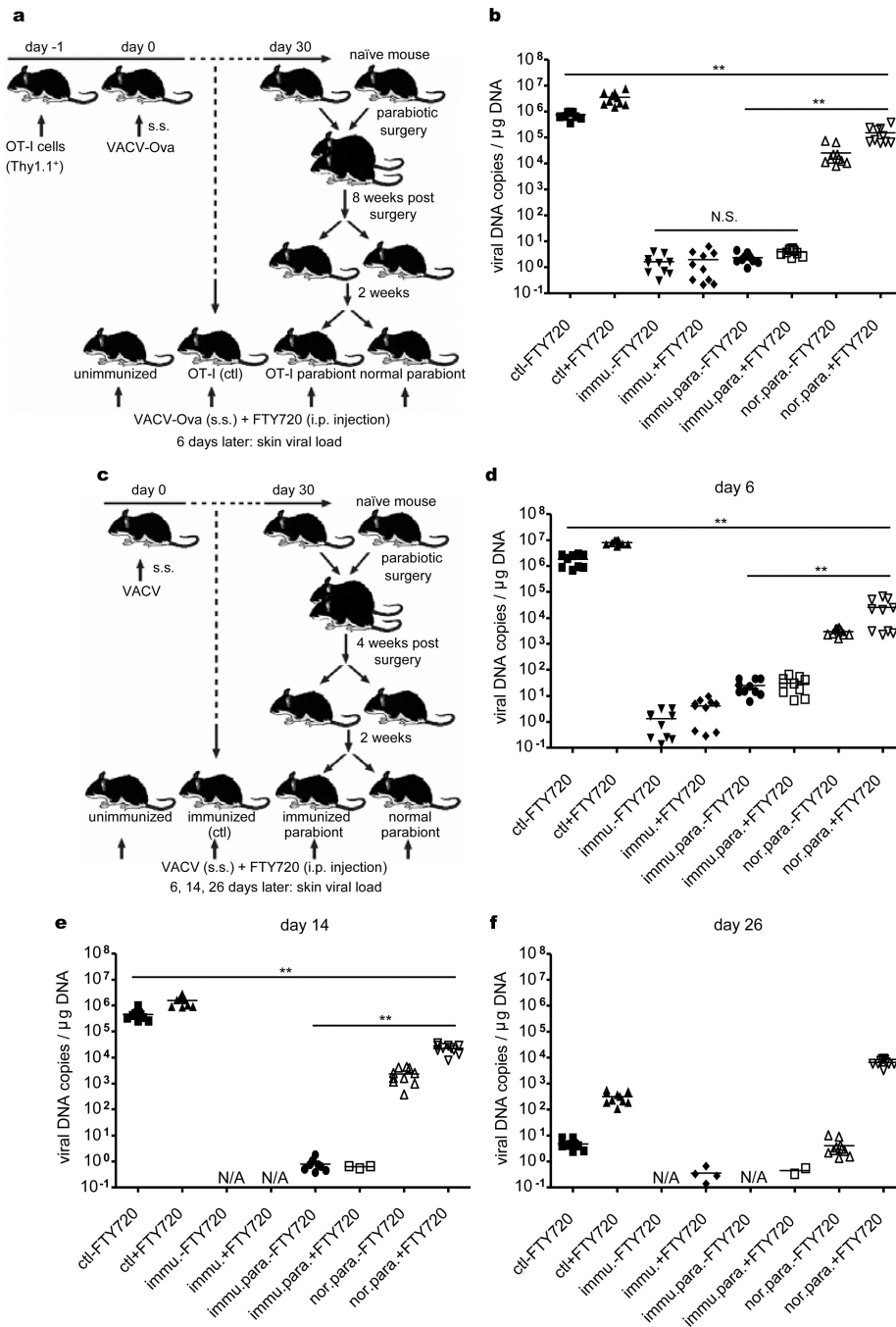
Figure 3. Skin CD8$^+$ T$_{RM}$ are superior to both antibody and T$_{CM}$ at protecting against re-infection

a, μMT mice with OT-I transfer and VACV-Ova skin infection were used to create OT-I : normal parabiotic mice as before. 8 weeks after surgery, parabiotic mice were separated. 2 weeks later, separated mice were challenged with VACV-Ova on the skin. Half mice were injected daily with FTY720. **b**, 6 days after challenge, skin viral load was assayed by qPCR. **c**, In separate experiments, μMT mice without OT-I transfer but with VACV skin infection were used to create immunized : unimmunized parabiotic mice. 4 weeks after surgery, the

same VACV skin challenge protocol was applied. **d-f**, 6, 14, or 26 days after challenge, viral load was assayed. The results from duplicate qPCR runs are plotted. Horizontal bars indicate the mean. Data are representative of two independent experiments (n = 5 mice/group). **, $P<0.01$; N.S., not significant.

Figure 4. Skin CD8^{+} T$_{RM}$ also accumulate in unimmunized site after skin infection and are highly effective at eliminating virus

a, $2{\times}10^6$ Thy1.1^{+} OT-I cells were intravenously transferred into Thy1.2[+] mice 1 day prior to $2{\times}10^6$ PFU VACV-Ova skin scarification (s.s.). The numbers of OT-I cells in infected and uninfected skin were enumerated over time. **b**, The left ears of OT-I-infused B6 mice were infected with VACV-Ova. 20 and 30 days later, some of mice were challenged with $2{\times}10^6$ PFU VACV-Ova on the tail and flank skin, respectively. All infection routes were s.s.. 30 days after challenge, Thy1.1[+] OT-I cells in uninfected right ears were examined. **c**, The percentages of Thy1.1[+] OT-I cells in uninfected right ears. **d**, The numbers of Thy1.1[+] OT-I cells in uninfected right ears. Error bars, s.e.m. **e**, μMT mice were infected with VACV either by s.s. on one ear or intraperitoneal (i.p.) injection. 7 or 30 days later, mice were challenge with VACV on both ears via s.s. route. Daily i.p. injection of FTY720 was performed. **f**, **g**, 6 days later, viral loads in both infected and uninfected ears were measured. The mean and s.d. from triplicate qPCR runs are plotted. Data are representative of three independent experiments (n = 5 mice/group). **, $P{<}0.01$.